

A High-Accuracy DOA-Based Localization Method: UAV Virtual Multiantenna Array

Jianqiao Cheng

Brussels School of Engineering
Université libre de Bruxelles (ULB)
Brussels, Belgium
Jianqiao.Cheng@ulb.be

Ke Guan

State Key Lab of Rail Traffic Control and Safety
Beijing Jiaotong University (BJTU)
Beijing, China
kguan@bjtu.edu.cn

François Quitin

Brussels School of Engineering
Université libre de Bruxelles (ULB)
Brussels, Belgium
fquitin@ulb.be

Abstract—Reliable location-aware services and corresponding localization techniques are essential in Unmanned Aerial Vehicle (UAV) communications. In this paper, localization technology based on Direction of Arrival estimation is proved to be promising for UAV channels due to limited angular spread in the air. Then, a method is proposed to estimate the direction of a ground radio-frequency transmitter by using a UAV equipped with a single antenna, which is critical when considering the form factor and computational capabilities of a UAV. By considering the received signal at several points along its trajectory, the receiver implicitly creates a virtual multi-antenna array, which can be used to estimate the direction of the transmitter. The first difficulty is estimating the relative positions of the UAV. The other main challenge is the Local Oscillator frequency offset between the transmitter and the UAV receiver, which adds an additional cumulative phase offset to the received signal at each antenna of the virtual array.

Index Terms—Direction Finding, DoA Estimation, Localization, Multi-antenna System, Radiogoniometry

I. INTRODUCTION

Estimation of the location of passive Radio Frequency (RF) sources (e.g., emitting radio, etc.) has been a subject of research for decades and plays a significant role in many applications, including radar and sonar processing, search and rescue missions, and wireless sensor networks [1]. Measurements used for passive localization can be classified into four categories: Time Of Arrival (TOA), Time Difference Of Arrival (TDOA), Direction Of Arrival (DOA), and Received Signal Strength (RSS) [2]. Also, in most cases, a basic assumption for passive localization is that the Line-Of-Sight (LOS) visibility exists between a transmitter and receiver, as the transmitter location estimates can be significantly biased due to multipath transmission and shadow fading [3]. While this assumption is rigid to guarantee in the ground communication channels (e.g., a dense urban environment) due to rich obstacles, the LOS path is easy to establish in the Air-To-Ground (ATG) channels, as scatters are limited in high altitudes [4]. In other words, the accuracy of localization services can be significantly improved by utilizing measurements from the sky, and Unmanned Aerial Vehicles (UAVs) are a promising platform to serve as an aerial localization node.

The investment in UAVs has surged in recent years due to their low cost, ease of on-demand deployment, and excellent

mobility. UAVs are widely used in various applications, including target reconnaissance, image acquisition, surveillance, and wireless communication [5]. Furthermore, as an essential part of the future Low Altitude Platform (LAP) communication system, UAV has tremendous amounts of excellent characteristics, such as the high probability of a LOS path, unencumbered by rough terrain and fewer reflections from obstacles on the ground [6]. Current studies are focusing on the UAV serves as a mobile terminal (e.g., base stations and relays), and the UAV serves as new aerial users that access the cellular network from the sky [7]. Alongside the enormous connectivity potential, reliable location-aware services are also essential in UAV-based communications. Therefore, localize ground users with UAVs is becoming an important topic and has drawn significant attention. For example, UAVs have been used to localize WiFi devices and GPS jammers [8].

Despite the high potential, performing localization with UAVs also has some drawbacks: UAVs also have limited payloads and flight times due to hardware and battery limits. Therefore, some localization methods are not suitable in UAV-based scenarios. For example, the TOA-based and TDOA-based localization systems usually require precise and consistent time synchronization, which is complex in UAV scenarios. Likewise, DOA estimation uses phase interferometry, i.e., the phase differences among the bearing measurements w.r.t. multiantenna array elements [9]. However, since UAVs are usually small, the consequent constraints on the size of the multiantenna array will lead to poor spatial resolution [2]. Ranging localization with RSS methods is attractive due to their intrinsic simplicity. However, its accuracy is usually not satisfactory. Therefore, a simple, cost-effective localization method using a minimum number of UAVs, without heavy hardware implementation and complex synchronization, is precious for the development of aerial RF localization.

In this work, we investigate the feasibility of DOA estimation with a UAV equipped with a single antenna only [10]. The unknown signal source to be located is referred to as the transmitter. The UAV is flying and carried with a single patch antenna (mounted facing downward), referred to as the receiver. While the UAV hovers overhead at a certain altitude, the receiver antenna receives the incoming signal consistently along the UAV's trajectory, as shown in Figure 1. Bearing

measurements are taken at fixed time intervals during the flight and are then processed to extract the phase difference at these observation points. Therefore, we implicitly create a *virtual Multiantenna Array* (VMA) in 3D space. Combining these bearing measurements with UAV's position, an estimate of the source's DOA (including azimuth angle and elevation angle) is obtained. The receiver antenna at each observation point can be considered a virtual antenna element in VMA. Like conventional multiantenna arrays, the element spacing should be smaller than the half wavelength of the carrier frequency to avoid aliasing effects.

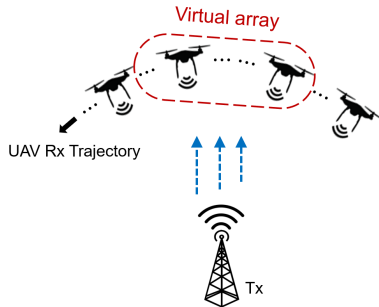


Fig. 1. UAV virtual array concept. Single UAV receiver equipped with one single antenna, moves and create a virtual array.

The difficulties of such a UAV-based VMA method are threefold: 1) The aerial channel between UAV stations and ground users differs significantly from conventional terrestrial channels, and the effect of aerial channel properties (e.g., angular spread) on DOA localization needs to be investigated. 2) The relative coordinates of UAV array elements are essential when calculating the array response vector that necessary for DOA estimation. 3) The concept of VMA is based on a consumption that the phase difference is only caused by the UAV movement. However, this is not the case in practice. As the Local Oscillator (LO) in transmitter and receiver has different frequency stability due to manufacturing tolerances and temperature variations [2], a LO offset usually appears and caused cumulative phase drifts for the received signal over time. Common RF devices usually equip with LOs that containing significant LO offset. For this reason, we provide two methods to compensate for the effect of LO offset, and their performance is tested in simulations.

In summary, the significance of our work lies in proving the feasibility of the VMA method with cheap, portable hardware that is already available in modern smartphones. Also, a UAV-based scenario provides a suitable, favorable propagation condition for VMA to show localization ability. Furthermore, by exploiting the potential of UAV's excellent mobility, our VMA system does not increase energy consumption or require multiantenna arrays. The results from simulations and experiments show that the VMA significantly outperforms the conventional localization algorithms in UAV-based scenarios in terms of localization accuracy and system simplicity.

Contributions: The main contributions of this paper are as follows.

- We proposed a technology to localize ground RF transmitters by creating a virtual multiantenna array with a single UAV platform. The proposed system is easy to implement for remote electronics.
- The spatial property of the ATG channel is studied with the ray-tracing method from a localization perspective. Our simulation results show that angular spreads at the UAV are minimal, which is beneficial for DOA-based localization due to limited power dispersion.
- The proposed system is implemented with simulations, and simulation results prove the feasibility of the VMA method.

The remainder of the paper is organized as follows. Section II provides a detailed spatial channel characteristics analysis of the ATG channel from a localization perspective. Section III proceeds with the design and system model of the VMA model. Two algorithms are provided to eliminate the bias introduced by LO offset. Section IV concludes this paper and presents our future work.

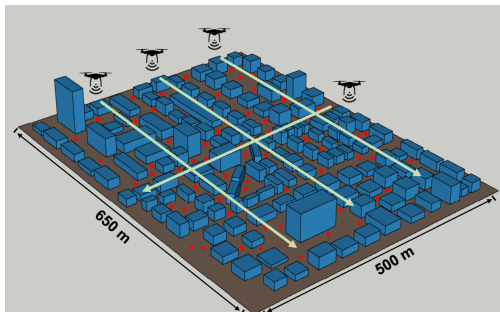
II. SPATIAL PROPERTY OF UAV CHANNEL

The estimation of the bearing angle is usually estimated based on antenna measurements with conventional array processing algorithms (e.g., Multiple Signal Classification (MUSIC), Beamforming). Nearly all of these algorithms assume that the source signal arrives at UAV with a discrete, distinct angle. This assumption leads to a signal subspace of low rank, and the low-rank property is exploited to find the impinging direction.

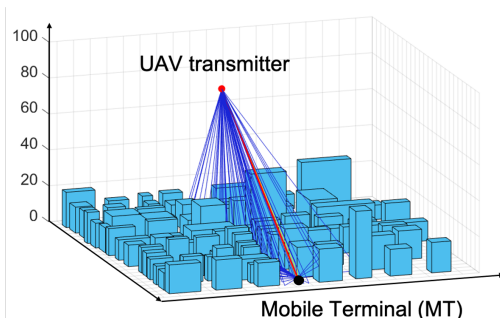
However, in actual spatial channels (e.g., a macro-cell), several replicas of the signal will be incident on UAV with multiple angles due to multipath propagation. More specifically, the signal that incident on UAV array may spatially be distributed (i.e., with an angular spread around a mean DOA) and no longer propagate along with a plane wave due to local scatters surrounding the ground transmitter. The angular spread usually denotes the standard deviation of DOAs from multipath, also indicates the power dispersion in the angular domain. Generally speaking, a large angular spread value will directly degrade the antenna array correlation, which gives rise to the inaccuracy of the DOA estimation; For small angular spread, it follows from the consistency that the mean DOA will only deviate slightly from the true DOA. These mismatches between the mean DOA and true DOA in the ground channel is well investigated in [11]. However, very limited research has thoroughly investigated similar spatial properties in UAV channels from a localization perspective to the best of our knowledge.

To ensure the effectiveness of DOA measurements in UAV-based localization, we investigate the spatial characteristics of the ATG channel with Ray-Tracing simulations. Given the purpose of localization, i.e., the UAV-based platform locates ground users according to their emitted signal, we consider the ground users serve as Mobile Terminals (MTs, emulating

a transmitter), the UAV serves as an aerial receiver (Rx), to locate ground MTs according to their emitted signal. Moreover, When the carrier frequency does not change (which is our case), the angular spreads in the uplink and downlink are equivalent due to the channel reciprocity. Therefore, although the signal travels from MT to UAV, the channel can still be referred to as the ATG channel.



(a) Ray-tracing simulation scenarios



(b) One example snapshot from ray-tracing simulations

Fig. 2. The Ray-tracing simulations. (a) The scenario contains 4 linear UAV trajectories, and 250 MTs randomly distributed on the ground. (b) An example from the RT simulation results. The solid red line represents the line-of-sight path, the blue lines represent all the multipath components, including reflected rays, scattered rays and diffracted rays.

Ray-tracing is a powerful map-based hybrid channel modeling approach to describe multipath effects for a given environment model and deployment configuration [12]. Our simulations are carried out by using CloudRT, the 3D ray-tracing software developed by Beijing Jiaotong University. In this work, we modeled a typical 3D urban city, with 137 buildings under different heights going from 5 m to 70 m. The total dimensions of the modeled terrain are 650 m by 500 m. The area has 250 ground MTs distributed uniformly over the whole map, and the MT height is set to 2 m above ground. The UAV is equipped with a downwards-facing patch antenna, and MTs are equipped with vertically-oriented dipole antennas. It is worth mentioning that the tilts of MTs antenna are randomly distributed but deviate no more than $\pm 45^\circ$ from the vertical direction. Both the UAV antenna and the MT antenna are vertically polarized with 0 dBi gain, and the transmission power is set to 0 dBm. The simulation is conducted by fixing the MT while changing the position of the UAV along four linear trajectories. Each trajectory has a length of 450 m and contains 50 UAV positions, with a

resolution of 9 m, as shown in Figure 2(a). Considering that Long-Term Evolution (LTE) is a reliable technology to support the required link performance of UAV networks [5], we set the carrier frequency at 2.6 GHz, corresponding to the LTE carrier frequencies. Moreover, the UAV altitude in simulations is conducted at 100 m.

The CloudRT software allows to simulate the direct ray between transmitters and receivers, first- and second-order reflections, diffracted rays along building edges, and diffuse scatterings on rough surfaces, as depicted in Figure 2(b). During the simulation, rays are collected, and then a Channel Impulse Response (CIR) is calculated by the software, including received power strength, phase, propagation time, angle of arrival, and angle of departure (for both azimuth and elevation). Also, the direct path between the UAV and MTs can be obstructed by obstacles; thus, we have a collection of the LOS and the Non-Line-Of-Sight (NLOS) cases. For the UAV altitude to be set to 100 m, we collected $250 \times 50 \times 4$ snapshots in total, containing 28626 LOS cases and 21374 NLOS cases. For each snapshot, the different Multipath Components (MPC) between the UAV and MT were recorded. These were used to determine the Azimuth-Of-Arrival (AOA) spread and the Elevation-Of-Arrival (EOA) spread. The Probability Density Function (PDF) of the angular spreads in the LOS scenario and the NLOS scenario are plotted in Figure 3, where the PDF function is used to specify the probability of an angular spread falling within a particular range of values.

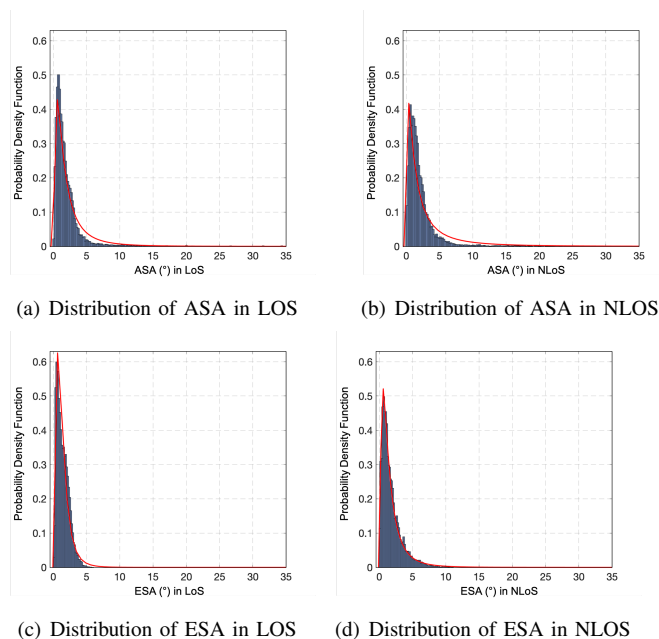


Fig. 3. Distributions of ASA/ESA in LOS scenarios and NLOS scenarios. The superimposed red curves are lognormal distributions used to model the PDF.

To better characterize the distribution of angular spreads at the UAV, the lognormal distribution is chosen to be the most appropriate function to fit the ASA and the ESA. For example, in LOS scenarios, the PDF of the ASA can be mathematically

expressed by:

$$f_{ASA}(x) = \frac{1}{\sqrt{2\pi x \sigma_{ASA}}} \exp \left[-\frac{(\ln x - \mu_{ASA})^2}{2\sigma_{ASA}^2} \right] \quad (1)$$

where μ_{ASA} and σ_{ASA} are the mean and Standard Deviation (STD) of the fitting PDF, respectively. The fitting of ESA is similar by replacing parameters μ_{ASA} , σ_{ASA} with μ_{ESA} , σ_{ESA} . The value of μ and σ for ASA/ESA spreads in both LOS and NLOS scenarios are provided in Table I.

TABLE I
LOGNORMAL MODELING PARAMETERS

Parameters	ASA		ESA	
	LOS	NLOS	LOS	NLOS
μ	0.42	0.52	0.15	0.24
σ	1.01	1.29	0.68	0.91

By comparing the PDF distribution and the established statistical model, the spatial multipath propagation characteristics can be observed as follows.

- The first observation from Figure 3 is that the ESA and ASA are distributed over a narrow range less than 10° (with an average angular spread around 2.5°), for both LOS and NLOS scenarios. These magnitudes are much smaller than the ESA and ASA in conventional 3D cellular channels, e.g., average ASA around 9° and average ESA around 15° in [13]. Such observations indicate that the spatial dispersion of received power at the UAV side is very limited, and all the multipath components arrived at the UAV with similar incident angles. Therefore, the power-weight mean AOA/EOA is a good representation of the real bearing to the ground MT.
- In Figure 3, the histograms for both ASA and ESA are steeper in the LOS scenarios than the NLOS scenarios. The μ and σ in LOS are also smaller than NLOS. Therefore, the angular spread in NLOS scenarios tends to be slightly larger than in the LOS scenarios. This phenomenon is expected and can be explained by the fundamental of angular spread: When scattered MPCs make a considerable contribution to the total received power, the angular spread will be large; When the LOS path is dominant among the received power, the angular spread will be small. In NLOS scenarios where the LOS path has been blocked by obstacles, the direct signal will be attenuated; Thus, MPCs will make more significant contributions in the total received power, caused a bigger angular spread in both azimuth and elevation domain.

The analysis above leads to the following conclusion. In urban environments, the angular spread at the UAV is minimal, which means the power dispersion at the UAV is very limited. Therefore, the DOA-based estimation has a great potential in UAV-based cellular networks to localize ground targets since the estimated DOA should be close to the true DOA.

III. UAV VIRTUAL MULTIAN TENNA ARRAY SYSTEM MODEL

A. UAV-based Virtual Array System

The system model of the virtual antenna array is following. We consider that a single transmitter broadcasts an RF signal periodically while the UAV-carried receiver is moving. The periodically transmitted RF signal in our system is in the form of digital data packets. Both the transmitter and the receiver know the preamble of the packets. Those preambles are defined by existing communication standards, e.g., the Primary Synchronization Signal (PSS) broadcast by the base stations in LTE standard [9].

As for the DOA localization, the unknown location of the stationary transmitter in three-dimensional Cartesian coordinates is represented by $s = [x, y, z]^T$ (the superscript T denotes the matrix transpose operator). The knowledge of UAV's location is represented by $s_i = [x_i, y_i, z_i]^T$ for $i = 1, \dots, N$. Here, i denotes the i th virtual array element along UAV's trajectory, and N represents the total number of these points. Generally, we can determine the location of s as long as we estimated the DOA, as seen from the UAV. The DOA, including the AOA φ and the EOA θ , is calculated by analyzing the phase difference in received packets. As the signal arrives at s_i from the far-field, the DOA at each observation point is considered the same.

Let us denote $s[m]$ the baseband representation of the transmitted packet preamble (for $m = 1, \dots, M$) and $r[n, m]$ the m -th baseband sample of the n -th received packet, which can be represented as:

$$r[n, m] = h[n, m] * s[m] \cdot e^{j(\phi_0 + 2\pi f_0(t_n + mT_s))} + \omega[n, m] \quad (2)$$

where $h[n, m]$ is the CIR, which provides temporal and spatial information and power of multipath components. The term ϕ_0 is the phase of the first received packet (which contains the phase offset and accumulated frequency offset at time t_0 between the transmitter and receiver front-ends), f_0 is the LO frequency offset between transmitter and receiver, t_n is the elapsed time between the initial packet and the n -th packet. The term T_s indicates the receiver sample time and $\omega[n, m]$ is an independent and identically distributed Gaussian noise with distribution $\omega[n, m] \sim \mathcal{CN}(0, \sigma^2)$. We assume that f_0 is constant during the observation interval at each interception position, which means the movement of receiver can not exceed a certain time limit, e.g. a few seconds. The term ϕ_0 is considered constant between multiple received packets [9].

In the following (unless otherwise stated), we will consider a narrowband LOS channel. The narrowband channel $h[n]$ when the receiver receives the n -th packet can be written as:

$$h[n] = \alpha \cdot e^{j\vec{\beta}(\varphi, \theta) \cdot \vec{r}[n]} \quad (3)$$

where α is amplitude of the channel, $\vec{\beta}(\varphi, \theta)$ is the wave vector, $\vec{r}[n]$ is the n -th virtual array coordinate when receiving the n -th packet relative to initial coordinate, which requires knowledge of the location of the UAV to within a small

fraction of the carrier wavelength. While the UAV flying at a fixed altitude (as will be considered in the following sections), the term $\vec{\beta}(\varphi, \theta) \cdot \vec{r}[n]$ can be developed as

$$\vec{\beta}(\varphi, \theta) \cdot \vec{r}[n] = \frac{2\pi}{\lambda} (x[n] \sin(\varphi) \cos(\theta) + y[n] \cos(\varphi) \sin(\theta) + z[n] \cos(\theta)) \quad (4)$$

where $x[n]$, $y[n]$, $z[n]$ represent the displacement of the receiver along the x-, y- and z- axis when receiving the n -th packet.

Combining equations (2) and (3), the full signal model can be written as:

$$r[n, m] = \alpha \cdot s[m] \cdot e^{j(\phi_0 + 2\pi f_0(t_n + mT_s) + \vec{\beta}(\varphi, \theta) \cdot \vec{r}[n])} + \omega[n, m] \quad (5)$$

The main difference between (5) and the received signal with conventional multi-antenna systems is twofold:

- 1) the frequency offset f_0 does not appear in conventional multi-antenna systems, since the signal is received on all antenna elements simultaneously;
- 2) the coordinates $\vec{r}[n]$ are perfectly known in a conventional multi-antenna system, since the array form factor is known by design.

In principle, the DOA estimation in the virtual array is only feasible after the LO phase offset caused by f_0 is eliminated, and the relative array element positions $\vec{r}[n]$ is known. The algorithms and techniques to deal with these two challenges are provided in the next sections.

B. Estimating the relative UAV Coordinates

While UAV is flying in the sky, its coordinates have to be known with an accuracy of a fraction of a wavelength. Current UAV-embedded GPS sensors usually far short from this requirement in higher frequency, but new generations of GNSS receivers in the near future may allow knowing the position of the UAV with such precision, especially since UAVs benefit from excellent satellite visibility. To address this challenge with off-the-shelf hardware, we add a 3D inertial measurement unit (IMU) on the UAV-mounted receiver, containing a combination of accelerometers, gyroscopes, magnetometers to measure angular velocity and linear acceleration with respect to the UAV's body coordinate frame. The relative position and orientation are characterized by the IMU readings through so-called dead-reckoning integration algorithms, with an Extended Kalman Filter (EKF) or an Unscented Kalman Filter (UKF) [9].

Due to the integration of biases in the IMU processing, the navigation solution obtained from IMU measurements will drift from the real trajectory, and the error of the navigation solution will increase over time. However, for the Wide-Sense Stationary Uncorrelated Scattering (WSSUS) assumption to hold [2], the time over which the UAV forms the virtual array would be short so that the navigation error incurred by the IMU is also limited. For typical UAV or vehicle speeds, the required movement duration is up to a few seconds.

C. Local Oscillator Frequency Offset Compensation

To estimate and compensate the LO frequency offset in (5), we proposed two methods, based on our previous research in [9], [10]. The first method is the Stop-and-Start (SaS) approach, where the UAV first stands still before starting to move. During standstill, only the LO frequency offset causes the phase in (5) to change with time and can therefore be easily estimated. This estimated value f_0 is then used during the movement of the UAV to compensate the LO frequency offset, where each received subsequent packet can be expressed as follows:

$$r'[n, m] = r[n, m] e^{-j2\pi f_0 \cdot (t_n + mT_s)} \quad (6)$$

The compensated signal $r'[n, m]$ contains the phase interferometry and can be used directly in conventional DOA estimation techniques. Although the SaS approach is straightforward and easy to implement. This method suffers from two disadvantages. The most obvious disadvantage is that the SaS approach restricts the movement of the UAV, as the UAV first needs to stand still before moving. The second disadvantage is that the LO frequency offset should not change too much between the moment that the UAV stands still to the moment that the receiver moves, which might not always be verified in practice (especially for low-quality LOs).

The other method is called the joint estimation approach, which has more advantages in practical applications for providing higher usage flexibility and no need to stop the UAV before the movement. In this method, we apply the MUSIC algorithm with an adapted signal model by including the LO phase offset into the steering vector of the virtual array. Let us rewrite (5) by stacking the N received packets in a column vector:

$$r[m] = a(f_0, \varphi, \theta) X[m] + \omega[m] \quad (7)$$

with the array steering vector lies in a three-dimensional space over f_0 , φ and θ and defined as:

$$a(f_0, \varphi, \theta) = \begin{bmatrix} e^{j(2\pi f_0 t_1 + \vec{\beta} \cdot \vec{r}[1])} \\ e^{j(2\pi f_0 t_1 + \vec{\beta} \cdot \vec{r}[2])} \\ \vdots \\ e^{j(2\pi f_0 t_1 + \vec{\beta} \cdot \vec{r}[N])} \end{bmatrix} \quad (8)$$

and $X[m]$ is constant for all virtual antennas, defined as

$$X[m] = \alpha_0 \cdot s[m] \cdot e^{j(\phi_0 + 2\pi f_0 m T_s)} \quad (9)$$

By developing the eigen-decomposition of the covariance matrix of $r[m]$, we can then estimate the nominal DOA and frequency offset $(\hat{f}_0, \hat{\varphi}, \hat{\theta})$ via a 3D-MUSIC search, and the corresponding MUSIC spectrum will exhibit the largest peak at the estimated DOA due to the orthogonality of the signal subspace and noise subspace [9].

D. Implementing VMA with Simulations

We have simulated the proposed virtual array system by using MATLAB software. We illustrate the DOA estimation

results under each of the two LO frequency offset compensation techniques in the next steps. The azimuth φ for each path in (4) is set to a random angle between 0° and 180° and the elevation θ is set to a random angle between 0° and 90° . The LO drift is simulated using the LO model described in [14].

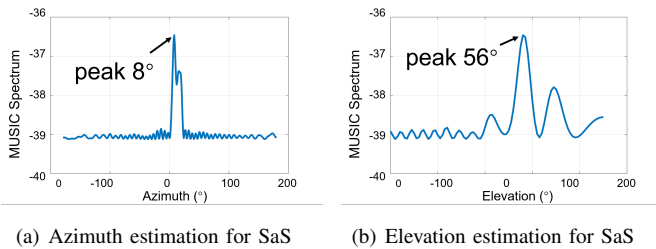


Fig. 4. Simulation results of the SaS estimation approach based on 2D MUSIC search (versus φ and θ , where f_0 is estimated in prior).

Figure 4 shows an example of the MUSIC spectrum of the SaS method after frequency offset compensation, which is used to estimate the azimuth and elevation angle simultaneously. In this snapshot, a clear peak is observed at azimuth 8° and elevation 56° , which is very close to the true DOA (12° for azimuth and 52° for elevation).

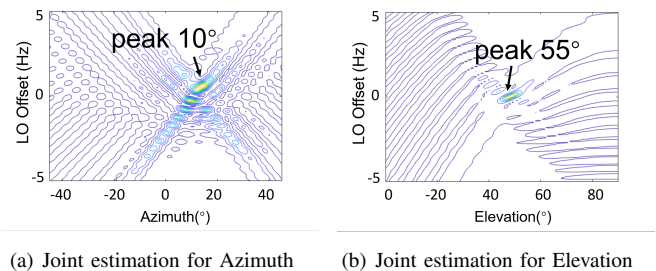


Fig. 5. Simulation results of the joint-estimation approach based on 3D MUSIC search (versus f_0 , φ , and θ).

Figure 5 presents an example of the joint-estimation method for the same snapshot in Figure 4. In this case, only the received packets during the UAV movement were used for processing. The peak of the spectrum indicates the estimated LO frequency offset f_0 , and also the estimated DOA (azimuth and elevation) corresponding to the peak. A clear peak can be identified at 10° for azimuth and 55° for elevation, close to the true DOA of 12° for azimuth and 52° for elevation as well.

IV. CONCLUSION AND FUTURE WORK

In this paper, the DoA-based localization is proved to be a suitable technology for UAVs to locate ground targets due to limited angular spreads for aerial nodes. A promising method is proposed to estimate the DOA of a ground RF transmitter with a UAV equipped with a single antenna. This method actively exploits the UAV movement, which can effectively be controlled and leveraged to obtain DOA estimations. By considering received packets along a planned trajectory, the UAV receiver creates a virtual multi-antenna array that can use conventional DOA estimation algorithms. In addition, we

propose two alternative methods to compensate for the local oscillator frequency offset between ground RF transmitters and UAV receivers. The feasibility of our UAV virtual array method is verified with simulations. Our future work will focus on evaluating and improving the proposed method's robustness and implementing the VMA system with UAV platforms and software-defined radios. The whole DoA estimation system will be tested in outdoor scenarios to investigate the effect of 1) the UAV movement states (height, trajectory length); 2) the hardware configurations (LO qualities, LO offset compensation methods); 3) the channel conditions (LOS visibility, SNR, multipath power).

REFERENCES

- [1] B. Ilya and T. Joseph, "Target detection and localization using mimo radars and sonars," *IEEE Transactions on Signal Processing*, vol. 54, no. 10, pp. 3873–3883, 2006.
- [2] J. Cheng, K. Guan, and F. Quitin, "Direction of arrival estimation with virtual antenna array: Observability analysis, local oscillator frequency offset compensation, and experimental results," *IEEE Transactions on Instrumentation and Measurement*, pp. 1–1, 2021.
- [3] J. Rodríguez-Piñero, T. Domínguez-Bolaño, X. Cai, Z. Huang, and X. Yin, "Air-to-ground channel characterization for low-height uavs in realistic network deployments," *IEEE Transactions on Antennas and Propagation*, vol. 69, no. 2, pp. 992–1006, 2021.
- [4] X. Cai, T. Izydorczyk, J. Rodríguez-Piñero, I. Kovács, J. Wigard, F. Tavares, and P. Mogensen, "Empirical low-altitude air-to-ground spatial channel characterization for cellular networks connectivity," *IEEE Journal on Selected Areas in Communications*, 2021.
- [5] Z. Yong, Z. Rui, and L. Joon, "Wireless communications with unmanned aerial vehicles: Opportunities and challenges," *IEEE Communications Magazine*, vol. 54, no. 5, pp. 36–42, 2016.
- [6] X. Cai, J. Rodríguez-Piñero, X. Yin, N. Wang, Ai B. Frølund P, and Y. Pérez, "An empirical air-to-ground channel model based on passive measurements in lte," *IEEE Transactions on Vehicular Technology*, vol. 68, no. 2, pp. 1140–1154, 2018.
- [7] X. Cai, I. Kovács, J. Wigard, and P. Mogensen, "A centralized and scalable uplink powercontrol algorithm in low sinr scenarios," 2020.
- [8] P. Adrien, D. Louis, L. Sherman, and E. Per, "Antenna characterization for uav based gps jammer localization," in *Proceedings of the 28th International Technical Meeting of The Satellite Division of the Institute of Navigation (ION GNSS+ 2015)*, 2015, pp. 1684–1695.
- [9] F. Quitin, P. De Doncker, F. Horlin, and TW. Peng, "Virtual multiantenna array for estimating the direction of a transmitter: System, bounds, and experimental results," *IEEE Transactions on Vehicular Technology*, vol. 67, no. 2, pp. 1510–1520, 2017.
- [10] J. Cheng, K. Guan, and F. Quitin, "Virtual multiantenna array for estimating the doa of a transmitter in uav-assisted networks," in *2020 IEEE 31st Annual International Symposium on Personal, Indoor and Mobile Radio Communications*. IEEE, pp. 1–6.
- [11] Y. Jin and B. Friedlander, "Detection of distributed sources using sensor arrays," *IEEE transactions on signal processing*, vol. 52, no. 6, pp. 1537–1548, 2004.
- [12] D. He, B. Ai, K. Guan, L. Wang, Z. Zhong, and T. Kurner, "The design and applications of high-performance ray-tracing simulation platform for 5g and beyond wireless communications: A tutorial," *IEEE Communications Surveys Tutorials*, vol. 21, no. 1, pp. 10–27, 2019.
- [13] R. Zhang, X. Lu, J. Zhao, L. Cai, and J. Wang, "Measurement and modeling of angular spreads of three-dimensional urban street radio channels," *IEEE Transactions on Vehicular Technology*, vol. 66, no. 5, pp. 3555–3570, 2016.
- [14] Z. Cristina and T. Patricia, "The clock model and its relationship with the allan and related variances," *IEEE transactions on ultrasonics, ferroelectrics, and frequency control*, vol. 52, no. 2, pp. 289–296, 2005.